International Journal of Nanomedicine

Dovepress
open access to scientific and medical research

Open Access Full Text Article

ORIGINAL RESEARCH

Zinc Oxide Particles Can Cause Ovarian Toxicity by Oxidative Stress in Female Mice Model

Yuanyuan Xu[1,2], Yu Zhao[2], Shanji Liu[2], Sidi Lv[3], Ling Chen[4], Wanzhen Wang[1], Yueying Feng[1], Fen Fu[1], Hengyi Xu[2]

[1]The Second Affiliated Hospital of Nanchang University, Nanchang, 330000, People's Republic of China; [2]State Key Laboratory of Food Science and Technology, Nanchang University, Nanchang, 330047, People's Republic of China; [3]Second Clinical Medical College, Nanchang University, Nanchang, 330006, People's Republic of China; [4]The First Affiliated Hospital of Gannan Medical University, Ganzhou, 341001, People's Republic of China

Correspondence: Fen Fu, The Second Affiliated Hospital of Nanchang University, No. 1 Mingde Rode, Nanchang, 330000, People's Republic of China, Tel +86-791-8631-1753, Email fu_fen@163.com; Hengyi Xu, State Key Laboratory of Food Science and Technology, Nanchang University, 235 Nanjing East Road, Nanchang, 330047, People's Republic of China, Tel +86-791-8830-4447-ext-9520, Fax +86-791-8830-4400, Email HengyiXu@ncu.edu.cn

Introduction: Zinc oxide nanoparticles (ZnO NPs) participate in all aspects of our lives, but with their wide application, more and more disadvantages are exposed. The goal of this study was to investigate the toxicity of ZnO NPs in female mice ovaries and explore its potential mechanism.

Methods: In this study, adult female mice were orally exposed to 0, 100, 200, and 400 mg/kg ZnO NPs for 7 days. We explored the underlying mechanisms via the intraperitoneal injection of N-acetyl-cysteine (NAC), an inhibitor of oxidative stress, and salubrinal (Sal), an inhibitor of endoplasmic reticulum (ER) stress.

Results: The results indicated that serum estradiol and progesterone levels declined greatly with increasing ZnO NPs dosage. Hematoxylin and eosin (HE) staining revealed increased atretic follicles and exfoliated follicular granulosa cells. Moreover, at the transcriptional level, antioxidant-related genes such as *Keap1* and *Nrf2*, and ER stress-related genes *PERK, eIF2α*, and *ATF4* were markedly upregulated. In addition, the expression of *Caspase12, Caspase9*, and *Caspase3*, which are genes related to apoptosis, was also upregulated in all ZnO NPs treatment groups. Serum malondialdehyde (MDA) content was remarkably up-regulated, whereas superoxide dismutase (SOD) activity was down-regulated. The 400 mg/kg ZnO NPs treatment group suffered the most substantial harm. However, ovarian damage was repaired when NAC and Sal were added to this group.

Conclusion: ZnO NPs had toxic effects on the ovary of female mice, which were due to oxidative stress, ER stress, and the eventual activation of apoptosis.

Keywords: zinc oxide nanoparticles, ovary, oxidative stress, endoplasmic reticulum stress, apoptosis

Introduction

Over the past few decades, nanoparticles have been widely used in agriculture,[1] cosmetics,[2] the garment industry[3] and medicine[4] because of their biocompatibility and their anti-corrosion, flame-retardant, and anti-ultraviolet abilities, as well as other special properties. One of the most commonly used nanoparticles is zinc oxide nanoparticles (ZnO NPs),[5] with an increased presence in the environment and an elevated likelihood of exposure via unintentional body contact. Many studies have reported on the harm caused by ZnO NPs, including damage to the digestive,[6] respiratory[7] and nervous systems,[8] owing to the induction of inflammatory responses and oxidative stress. Therefore, biosecurity with respect to ZnO NPs needs greater attention.

As an important part of toxicology, toxicity to the female reproductive system is under intense scrutiny. Infertility affects approximately 16% of couples worldwide,[9] with female factors accounting for half of these cases.[10] The ovary is one of the most critical organs in the female reproductive system. It is the site of oocyte maturation and release[11] as well as the site of the secretion of sex hormones like estrogen and progesterone, which are critical to pregnancy.[12] Ovarian health is easily affected by environmental factors such as air pollution, heavy metals, toxic chemicals, or nanoparticles.[13]

Received: 16 May 2022
Accepted: 4 October 2022
Published: 19 October 2022

Graphical Abstract

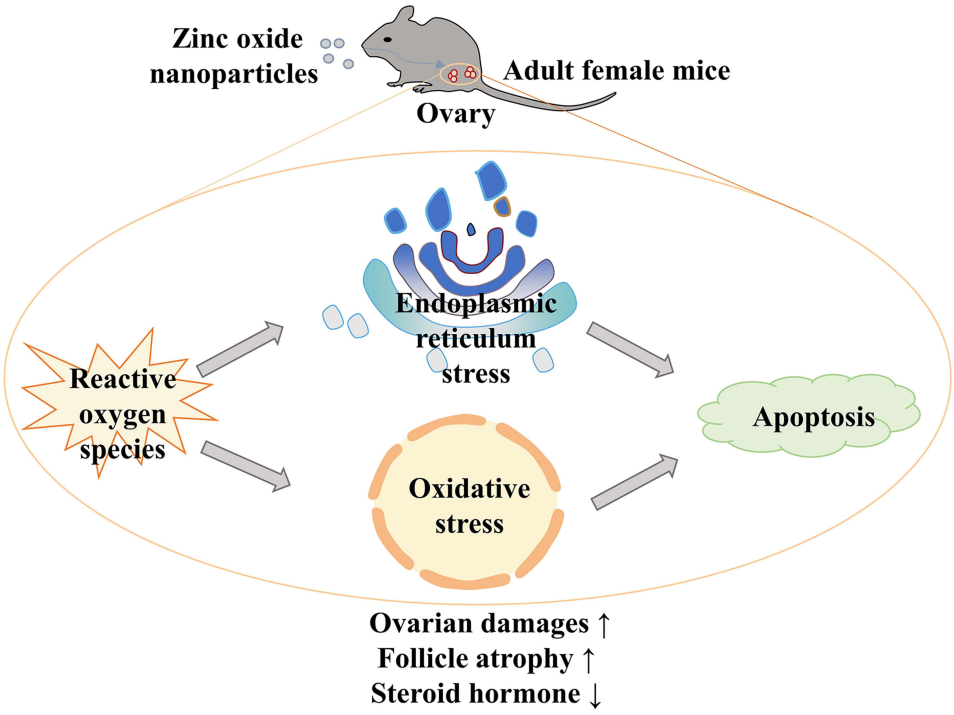

Nanoparticles enter the body via inhalation or ingestion and are then absorbed into the bloodstream, where they are finally deposited in secondary organs, including the ovaries, where they can cause varying types of damage.[14] In vivo, the sonic hedgehog signaling pathway is activated and causes the apoptosis of ovarian cells after exposure to ZnO NPs.[15] The toxicity of ZnO NPs in mouse ovarian cells has also been confirmed in vitro.[16]

Studies have indicated that the oxidative stress caused by reactive oxygen species (ROS) is involved in the process of toxicity owing to nanoparticles.[17] In some in vitro and in vivo experiments, ZnO NPs trigger oxidative stress pathways, resulting in tissue and cell damage.[18,19] The endoplasmic reticulum (ER) stress response has recently been identified as a potential early indicator of ZnO NPs exposure.[20] As an organelle, the ER is vital in protein construction and folding into appropriate tertiary structures.[21] When cells are triggered by external stimuli such as ZnO NPs, the amount of unfolded proteins in the ER lumen increases, disrupting ER homeostasis and producing ER stress to relieve the pressure on the ER.[22] Long-term ER stress may induce the activation of apoptotic signals, leading to tissue and organ damage.[23] In pregnant mice, ER stress can be activated by ZnO NPs, leading to developmental abnormalities in offspring and miscarriages.[24] In male mice, ZnO NPs cause testicular loss and sperm abnormalities via the activation of ER stress and apoptosis.[25] These data show that oxidative stress and ER stress may be involved in ZnO NPs-induced reproductive system damage. However, whether the ovarian damage in female mice caused by ZnO NPs is related to oxidative stress or ER stress is still unclear.

In this research, we evaluated the negative effects of ZnO NPs on the ovaries of female mice and used N-acetyl-cysteine (NAC) and salubrinal (Sal) to explore the potential mechanisms of toxicity. The adverse effects caused by different doses of ZnO NPs were evaluated by analyzing changes in ovarian coefficient, pathology, serum sex hormone levels, and Zn accumulation in tissues. We added inhibitors to the dose group in which ZnO NPs caused the most damage. We further investigated the potential mechanisms of ZnO NPs toxicity by analyzing the expression of genes and proteins linked to oxidative stress, ER stress, and apoptosis.

Materials and Methods

Material and Animal Treatment

Xiya Reagent, LLC (Chengdu, China) provided ZnO NPs powder. The characterization of the ZnO NPs has been reported in our previous research.[26,27] In general, Scanning Electron Microscopy micrographs showed that the diameter of ZnO NPs was about 27.5 ± 4.1 nm and the shape was spherical. Before the experiment, ZnO NPs powder was mixed with sterile water, placed in the ultrasonic instrument for 30 min, and then swirled for 1 min.

Healthy female C57BL/6 mice (weight 18±2 g) were provided by Hunan SJA Laboratory Animal Company (Hunan, China). The temperature in the animal room was controlled at 20–25 °C, the humidity was set at 40%–50%, the dark and light cycle was 12 h, and the padding was changed every 2 days. All experiments were authorized by Nanchang University's Animal Care Review Committee (authorization number: 0064257) and conducted in strict conformity with China's Guidelines for the Ethical Review of Laboratory Animal Welfare (GB/T35892-2018). Before the experiment, all animals were acclimated for 7 days on normal maintenance feed. Then, the mice were subdivided into four groups at random according to the dose of ZnO NPs: 0 (the control group), 100, 200, and 400 mg/kg (n =7 /group). The mice were orally administered after the preparation of ZnO NPs with different concentrations for 7 days. The control group was given the equivalent amount of sterile water. Body weight was monitored during the experiment. The mice were sacrificed after the last ZnO NPs treatment for 24 h. Blood was collected immediately by removing their eyeballs and stored at 4 °C. Then, the mice were carefully anatomized, and their ovaries were removed and saved.

NAC and Sal Supplementation

Forty female C57BL/6 mice (weight 18 ± 2 g) were divided into four groups at random: the control, 400 mg/kg ZnO NPs, 400 mg/kg ZnO NPs + 100 mg/kg NAC, and 400 mg/kg ZnO NPs + 1.5 mg/kg Sal treatment groups (n= 10 / group). NAC and Sal (MedChemExpress, USA) were injected intraperitoneally at 30 min after the gavage administration of 400 mg/kg ZnO NPs. Mice in the control group were given sterile water. The experiment was carried out for 7 days. Body weight was monitored daily. As mentioned above, the serum and ovaries were collected and kept at − 80°C.

The Histopathological Studies of the Ovary

The negative effects of ZnO NPs on the ovary were visualized by hematoxylin and eosin (HE) staining. After collecting the blood, the ovaries were removed and treated with 10% paraformaldehyde. The ovaries were fixed and then dehydrated in graded ethanol before being embedded in paraffin. The paraffin blocks were cut into 5 microns thick slices and flattened on a slide before being stained with hematoxylin and eosin and sealed with a cover glass. The changes in ovarian morphology were observed by an optical microscope at 200× and 400× magnifications.

Determination of Estradiol and Progesterone in Serum

Ovarian function was evaluated by measuring serum estradiol and progesterone levels. The serum was separated by centrifuging at 4000 r/min for 10 min after the whole blood was refrigerated at 4°C for 4 h. The mouse estradiol and progesterone ELISA kits were used for the determination. According to the instructions of the kits (YSRIBIO, Shanghai), the absorbance was detected at 450 nm with the enzyme label instrument (Thermo Scientific, USA). The standard material in the kit was used to establish a standard curve and calculate the sex hormone levels.

Determination of Total Zn Content in Ovary

The pre-treatments of the sample were referred to in the previous report.[28] Specifically, about 0.05 g of ovarian tissue was digested with 300 μL HNO_3 and 100 μL $HClO_4$ in a water bath at 95 °C for 2 h. The liquid was transferred to a 10 mL centrifuge tube after digestion, and ultra-pure water was added until a volume of 5 mL was reached. The Zn concentration was analyzed by Inductively Coupled Plasma-Atomic Emission Spectrometry (ICP-AES; Perkin Elmer Instruments, USA, 15005225). According to the weight of the samples and the measured concentration, the total Zn content in the ovary can be calculated.

Real-Time Quantitative PCR (RT-qPCR)

Total RNA from the ovary was isolated and reverse transcribed into cDNA according to the techniques described in the previous work.[29] Primer Express Software (Applied Biosystems, Foster City, CA, USA) was used to design the primers, which were then manufactured by TSINGKE Biological Technology (Beijing, China). Table S1 contains the primer sequences. The Agilent AriaMx Real-Time PCR Program (Agilent Technologies, USA) was used to operate RT-qPCR. The fluorochrome was TB Green II (TAKARA, Japan). The process was as follows: 95°C for 30s, then 40 cycles of 95°C for 5s, 60°C for 1 min, and 72°C for 30s. The $2^{-\Delta\Delta Ct}$ method was used to compute gene expression fold changes. *β-actin* was used as the internal reference.

Immunohistochemistry Analysis (IHC)

The paraffin sections of ovarian tissue were soaked in xylene and alcohol for dewaxing. An appropriate amount of EDTA buffer was used to repair antigens. Then the sections were incubated in 3% hydrogen peroxide at room temperature for 15 min to inhibit endogenous peroxidase. The goat serum covered the paraffin sections for 30 min. After overnight incubation with primary antibody against JNK (1:200, 24164-1-AP, Proteintech, Wuhan) at 4°C, the slices were incubated with HRP-marked secondary antibody (GB23303, Servicebio) for 30 min at 37°C. Diaminobenzidine (DAB) was used to develop the sections, and the nuclei were re-stained with hematoxylin. Then the slices were dehydrated in alcohol and xylene. Finally, the sheet is sealed with neutral gum and dried. IHC was quantified with IMG software based on a previous study.[30]

Immunofluorescence Assay (IF)

As described in the IHC section, paraffin sections of ovarian tissue were dewaxed, put in EDTA buffer to repair antigens, and then in goat serum to reduce non-specific staining. After overnight incubation with primary antibody against Caspase3 (1:200, 19677-1-AP, Proteintech, Wuhan) at 4°C, the slices were treated with fluorescent secondary antibody (1:100, BA1032, Bode Biological Engineering, Wuhan) for 60 min at 37°C. To redye the nucleus, the slices were incubated in 4',6-diamidino-2-phenylindole (DAPI) for 5 min in the dark before being sealed with the sealing solution. Image J software was used to quantify the mean fluorescence intensity.

Detection of Malondialdehyde (MDA) and Superoxide Dismutase (SOD) in Serum

The kits were purchased from Jiancheng Bio-tech Co. Ltd. (Nanjing, China). The content of MDA (A003-2) and SOD activity (A001-3-2) in serum were detected following the instructions.

Statistical Analysis

All measurements were made three times and analyzed by IBM SPSS Statistics 26 software. The final results were represented by mean ±SD. Differences between groups were statistically analyzed by one-way ANOVA. A significant difference is indicated by $P< 0.05$. The following nomenclatures: *$P< 0.05$, **$P < 0.01$, ***$P < 0.001$ (versus the control group) and $^{\#}P< 0.05$, $^{\#\#}P < 0.01$, $^{\#\#\#}P < 0.001$ (versus the 400 mg/kg ZnO NPs treatment group) were used to state significant differences between the investigated groups.

Results

ZnO NPs Damaged Ovarian Structure and Function

Changes in body weight and ovarian coefficient (ovarian weight [mg]/ body weight [g]) reflected the damaging effects of ZnO NPs to some extent. The body weights of mice in all experimental groups were not remarkably different from those of the control group after 7 days of exposure (Figure 1A). The ovarian coefficient decreased substantially in the 400 mg/kg ZnO NPs treatment group, but did not change remarkably in the 100 and 200 mg/kg ZnO NPs treatment groups, and showed an overall decreasing trend (Figure 1B). Pathological changes in ovarian tissues were assessed using HE staining (Figure 1C). Among the mice in the control group, the follicle structure was complete, the zona pellucida and corona radiata were clearly visible, the granulosa cells were neatly arranged, and the oocyte membrane was intact. However, the number of atretic follicles in the

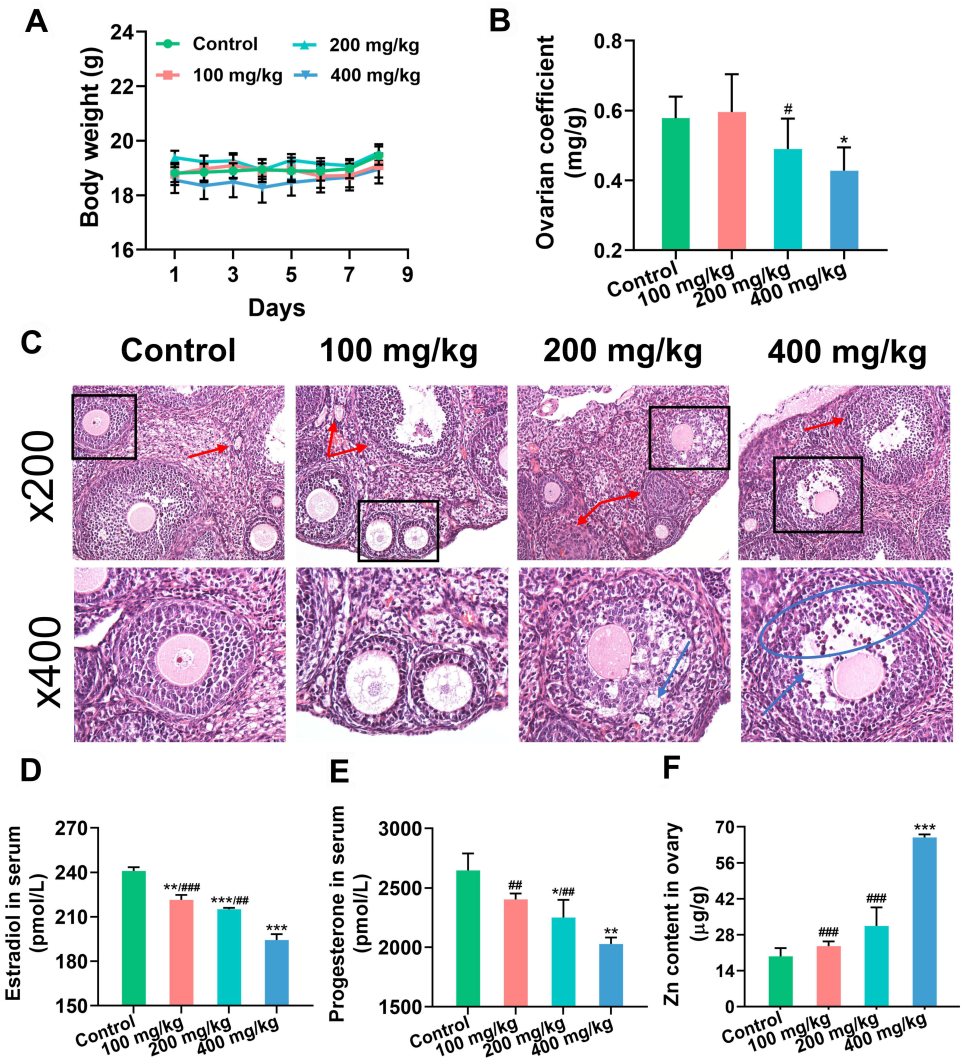

Figure 1 Changes of ovarian structure and function. (**A**) Body weight. (**B**) Ovarian coefficient. (**C**) Pathological changes of ovary. Red arrow: atretic follicle; blue arrow: shedding of granulosa cells; blue circle: disarray of granulosa cells; black square: localized enlargement. Magnification: ×200 and ×400. (**D** and **E**) The levels of estradiol and progesterone in serum. (**F**) Concentration of Zn in ovary. Ovarian coefficient = ovarian weight (mg)/ body weight (g). *P< 0.05, **P < 0.01, ***P < 0.001: ZnO NPs treatment groups versus the control group; $^{\#}$P< 0.05, $^{\#\#}$P < 0.01, $^{\#\#\#}$P < 0.001: the 100 mg/kg and 200 mg/kg ZnO NPs treatment groups versus the 400 mg/kg ZnO NPs treatment group.

ovary of mice increased after treatment with 100 mg/kg ZnO NPs, but the follicle structure was not remarkably damaged. Granulosa cells in the 200 mg/kg group were disordered and their exfoliation could be seen. The zona pellucida and corona radiata in the 400 mg/kg ZnO NPs treatment group were incomplete, more granulosa cells were exfoliated, and the oocyte membranes were uneven. Ovarian function was assessed according to serum steroid hormone levels. The serum levels of estradiol and progesterone decreased gradually with increasing ZnO NPs dosage compared with the control group. Considerable differences in estradiol and progesterone levels were found between the 100 or 200 mg/kg ZnO NPs treatment groups and the 400 mg/kg ZnO NPs group. (Figures 1D and E). Overall, the 400 mg/kg ZnO NPs treatment group caused the most structural and functional damage to the ovaries. As shown in Figure 1F, Zn content showed an upward trend and was prominently increased in the ovary of mice in the 400 mg/kg ZnO NPs treatment group ($P < 0.001$).

Expressions of Genes and Proteins Related to Oxidative Stress, ER Stress, and Apoptosis were Altered by ZnO NPs

As shown in Figure 2, ZnO NPs altered gene expression in antioxidant pathways. The expression of Kelch-like ECH-associated protein 1 (*Keap1*) was only prominently downregulated in the 400 mg/kg ZnO NPs treatment group, whereas

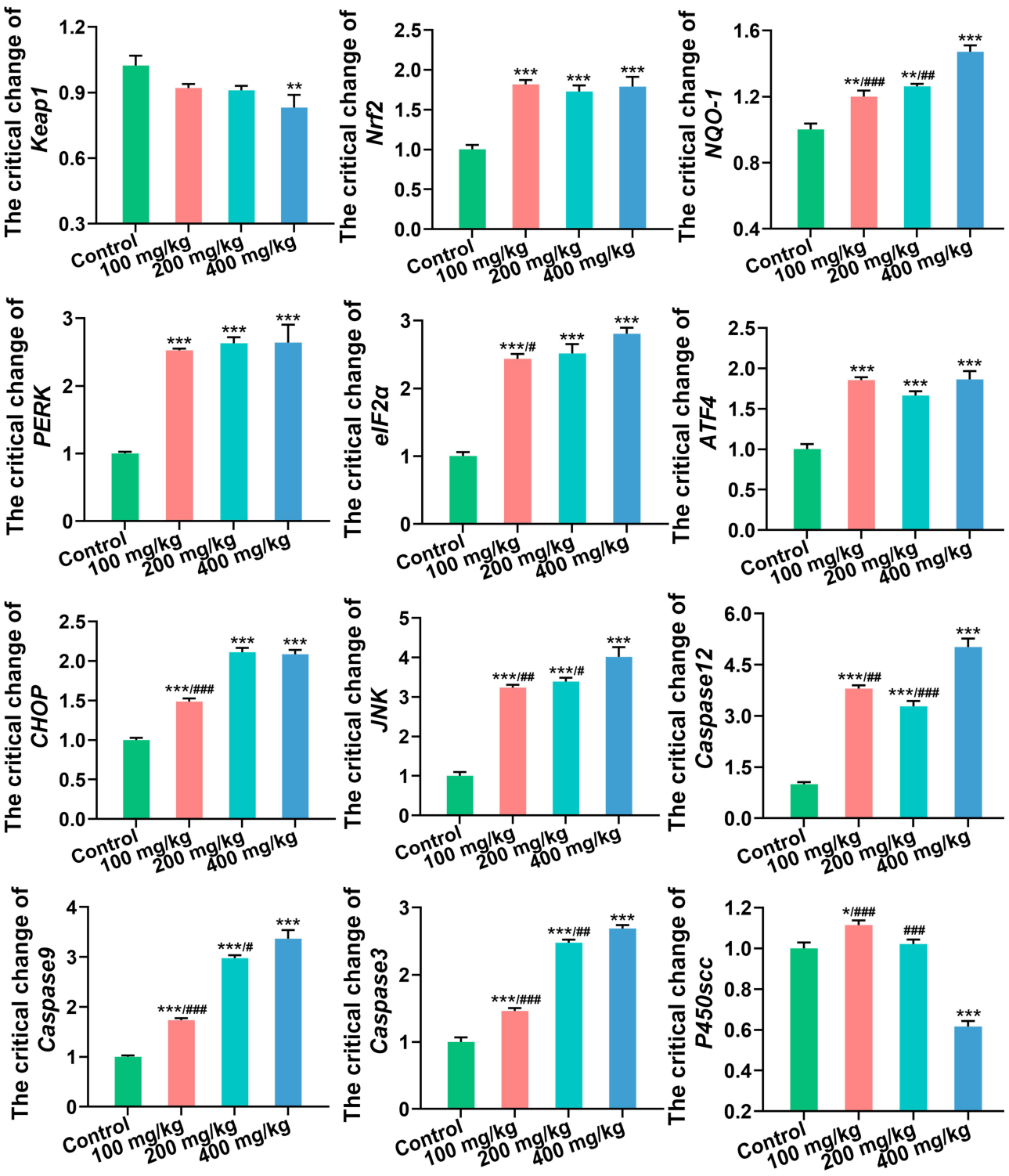

Figure 2 The expression levels of genes related to oxidative stress, ER stress, apoptosis and steroid hormone synthesis in ovary. *P< 0.05, **P < 0.01, ***P < 0.001: ZnO NPs treatment groups versus the control group; #P< 0.05, ##P < 0.01, ###P < 0.001: the 100 mg/kg and 200 mg/kg ZnO NPs treatment groups versus the 400 mg/kg ZnO NPs treatment group.

the expression of nuclear factor erythroid 2-related factor 2 (*Nrf2*) and NAD(P)H quinone oxidoreductase 1 *(NQO-1*) was considerably upregulated in all ZnO NPs treatment groups, especially in the 400 mg/kg ZnO NPs treatment group. Compared with the control group, the expression of genes related to ER stress was also prominently upregulated in the ZnO NPs treatment groups. Among them, eukaryotic translation initiation factor 2α (*eIF2α*), CCAAT/enhancer binding

protein homologous protein (*CHOP*), and c-Jun N-terminal kinase (*JNK*) were upregulated in a dose-dependent manner. Moreover, as key genes in apoptotic pathways, the expressions of *Caspase12, Caspase9*, and *Caspase3* were also considerably upregulated with a dose gradient. Finally, the expression of steroid hormone biosynthesis-related gene cholesterol side chain cleavage enzyme Cyp11a1 (*P450scc*) was overtly downregulated in the 400 mg/kg ZnO NPs treatment group.

At the protein level, JNK and Caspase3 expression were observed using IHC (Figures 3A and C) and IF (Figures 3B and D) respectively. Compared with the control group, JNK expression increased gradually with increasing ZnO NPs dose, and Caspase3 was only increased in the 400 mg/kg ZnO NPs treatment group.

Serum malondialdehyde (MDA) content was substantially up-regulated, whereas superoxide dismutase (SOD) activity was down-regulated with the increase in ZnO NPs dosage (Figures 3E and F).

NAC and Sal Repaired Damage to Ovarian Structure and Function

The ovarian coefficient was substantially increased after treatment with inhibitors (Figure 4B). In addition, the pathological sections showed that the follicular structure was complete, granulocytes were arranged in order, and atretic follicles were fewer (Figure 4A). Moreover, NAC or Sal supplementation remarkably increased the serum estradiol and progesterone levels compared with the 400 mg/kg ZnO NPs treatment group (Figures 4C and D).

ZnO NPs Damaged Ovary via Oxidative Stress and ER Stress

At the transcriptional level, the expression of *Keap1* in the antioxidant pathway was upregulated, and the expression of *Nrf2* and *NQO-1* was markedly downregulated after NAC and Sal supplementation compared with the 400 mg/kg ZnO NPs treatment group (Figure 5). Except for the relative expression levels of *eIF2α* and activating transcription factor 4 (*ATF4*) in the NAC group, the expression of other genes in the ER stress and apoptosis pathways was remarkably downregulated. Furthermore, *P450scc* expression showed an obvious upregulation trend (Figure 5). However, the expression levels of *PERK, eIF2α, ATF4, CHOP, JNK* and *Caspase3* in the inhibitor groups were still significantly higher than those in the control group.

At the protein level, the expression levels of JNK (Figures 6A and B) and Caspase3 (Figures 6C and D) were substantially decreased in both inhibitor groups.

Serum MDA content in serum was significantly downregulated and SOD activity was markedly upregulated after the inhibitors supplied were compared with the 400 mg/kg treatment group (Figures 6E and F).

Discussion

Considering the widespread use of ZnO NPs in daily life, this study aimed to explore the potential toxic effects of ZnO NPs on the ovary of female mice. The dosage selection was based on the study by Shen et al[31] and the standard set by the European Union. According to the European Committee for Standardization, the maximum daily intake of ZnO based on the 70 kg body weight of an adult is 0.45 mg/kg. The safety factor for investigating a substance's toxicity is usually 100 −1000 times. Our ZnO NPs dosage is within this range. Although the body weight of mice did not change considerably after the intragastric administration of ZnO NPs, the declining ovarian coefficient showed that ZnO NPs damaged the ovary. The same trend was reported by Liu et al, who studied the damage caused by ZnO NPs to neuronal factors and neuroendocrine cells in the ovary of hens.[32] Tang et al orally administered ZnO NPs to male mice and found that the relative epididymis weight began to decrease remarkably in the low-dose group (50 mg/kg), possibly because of the different sensitivity of different organs to ZnO NPs.[25]

The ovary is an important reproductive and endocrine organ. Follicular atresia is normal in mammals and occurs in about 99% of follicles.[33] However, increased atresia can result in impaired ovarian function. One study reported that atretic follicles in the ovaries of rats increased gradually with the increase in ZnO NPs dosage,[34] which showed a pattern similar to the results of our study. Follicular development and maturation are accompanied by the secretion of sex hormones.[35] Estradiol and progesterone are the most important sex hormones in women, and their serum levels reflect ovarian function to a certain extent. P450scc plays a vital function in the manufacture of ovarian steroid hormones, which can convert cholesterol into pregnenolone to produce estradiol and progesterone. Several studies have reported that the

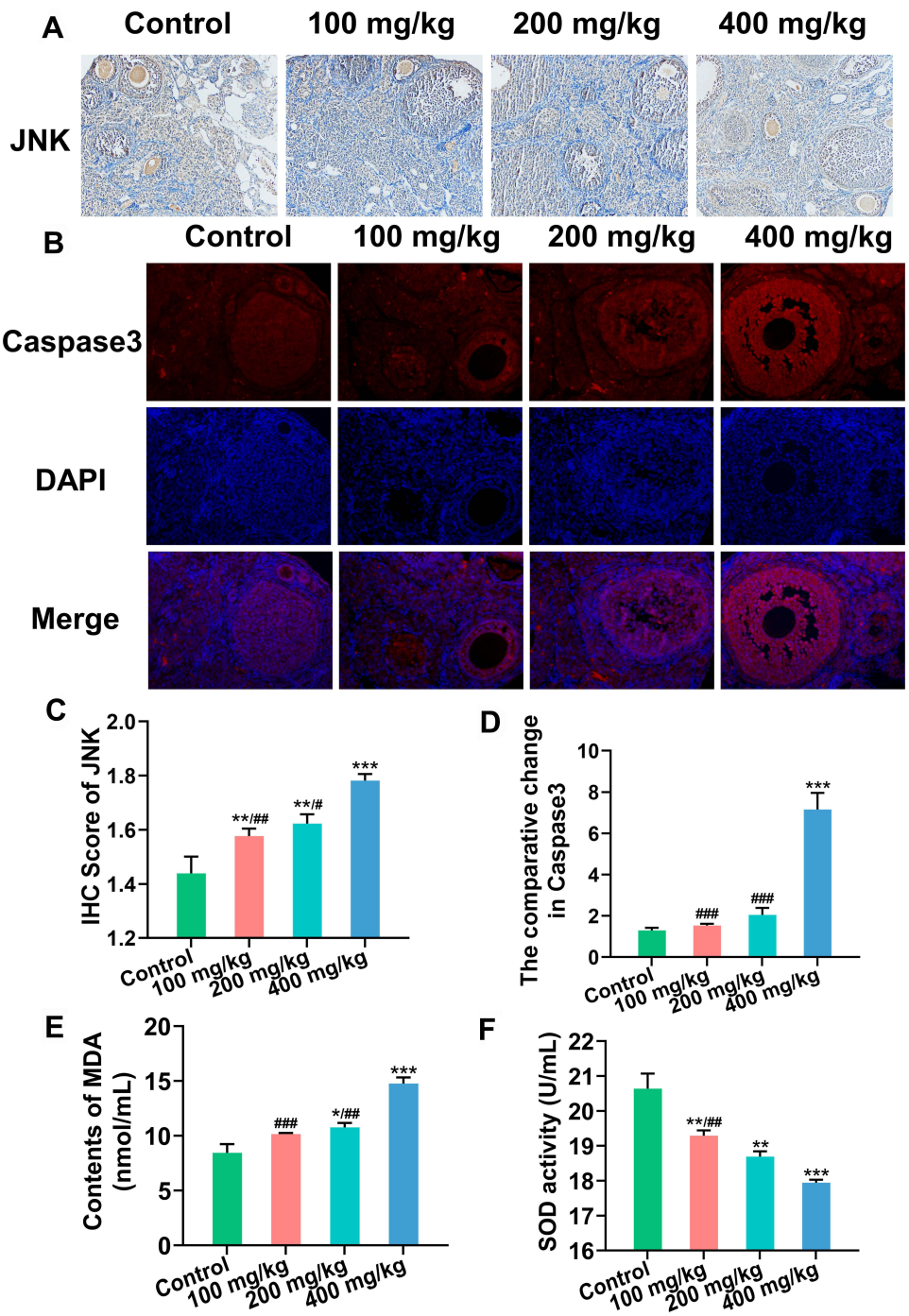

Figure 3 Protein expression of JNK and Caspase3 in ovary. (**A**) JNK expression detected by immunohistochemistry (IHC) (Magnification: ×200). (**B**) Caspase3 expression detected by immunofluorescence (IF) (Magnification: ×200). Blue: DAPI, red: Caspase3. (**C** and **D**) Semiquantitative analysis of JNK and Caspase3. (**E**) Content of MDA in serum. (**F**) SOD activity in serum. *P < 0.05, **P < 0.01, ***P < 0.001: ZnO NPs treatment groups versus the control group; #P< 0.05, ##P < 0.01, ####P < 0.001: the 100 mg/kg and 200 mg/kg ZnO NPs treatment groups versus the 400 mg/kg ZnO NPs treatment group.

activation of oxidative stress and ER stress can inhibit the synthesis of steroid hormones by downregulating *P450scc*.[36,37] In this study, the damaged ovarian function was reflected by increased atresia and considerably lower serum levels of sex hormones. It may be related to the downregulation of *P450scc*. These results were confirmed by Hong et al.[38] However, in the study of Liu et al, 30 nm ZnO NPs had no remarkable effect on sex hormones in adolescent hens, which is possibly due to the smaller dosages they used (25, 50 and 100 mg/kg).[32]

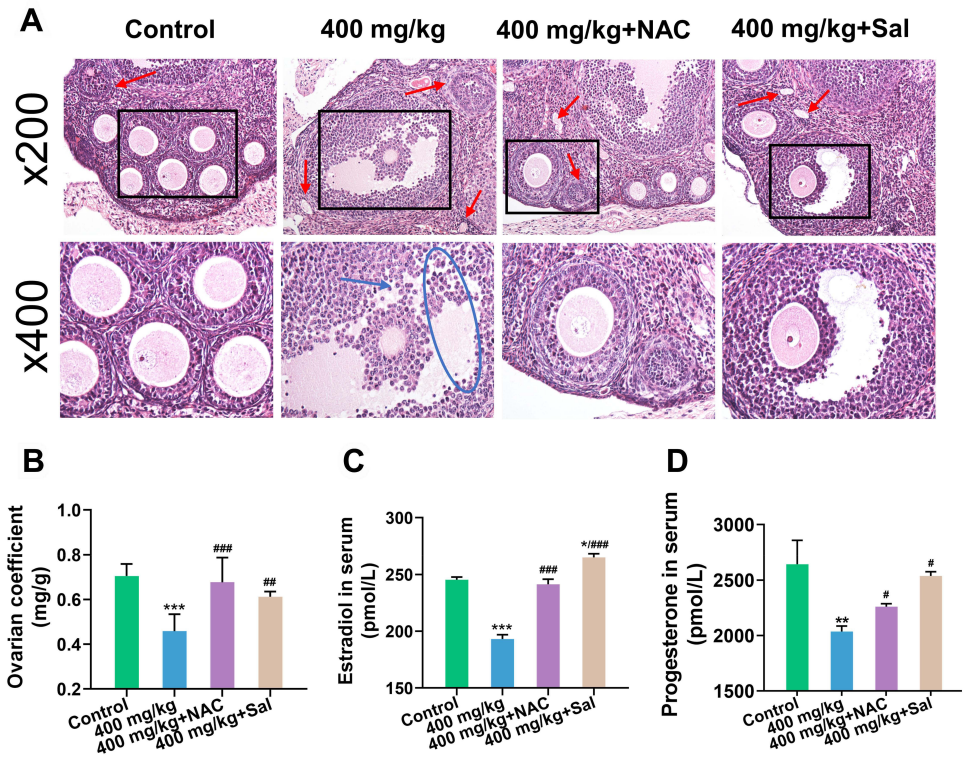

Figure 4 Changes of ovarian structure and function after the supplementation of NAC and Sal. (**A**) Pathological changes of ovary. Red arrow: atretic follicle; blue arrow: shedding of granulosa cells; blue circle: disarray of granulosa cells; black square: localized enlargement. Magnification: ×200 and ×400. (**B**) Ovarian coefficient. (**C** and **D**) The levels of estradiol and progesterone in serum. Ovarian coefficient = ovarian weight (mg)/ body weight (g). *P < 0.05, **P < 0.01, ***P < 0.001: the 400 mg/kg ZnO NPs treatment group and the inhibitor groups versus the control group; #P< 0.05, ##P < 0.01, ####P < 0.001: the inhibitor groups versus the 400 mg/kg ZnO NPs treatment group.

Zn accumulation in the ovary is a manner by which ZnO NPs produce toxicity.[39] The findings in our study were comparable to those of a previous study, which found that mice in the 400 mg/kg ZnO NPs treatment group had a considerably higher Zn level in their uterus during early pregnancy.[40] Moreover, we found that the 100 and 200 mg/kg ZnO NPs treatment groups had similar Zn levels as the control group, but the structure and function of the ovary were impaired in both groups, indicating that certain signaling pathways were potentially activated.

The accumulation of nanomaterials in vivo could increase ROS production.[41] ROS production can be induced in a variety of ways. For ZnO NPs, it may be related to surface catalytic reactions. In short, special catalytic reactions occur between O_2 and surface defects on ZnO NPs, resulting in ROS formation. The absence of light exposure, such as in the body, may lead to more potent toxicity.[42] ROS production is followed by the activation of the antioxidant pathway Keap1/Nrf2.[43] Nrf2 is normally found inactive in the cytoplasm, bound to its inhibitor protein, Keap1. When ROS stimulates cells, Nrf2 is uncoupled from Keap1. Then, Nrf2 is activated and transported into the nucleus, where it modulates the transcriptional activity of downstream molecules such as phase II metabolic enzymes and antioxidant enzymes, and plays the role of antioxidants. Various downstream target proteins can be activated after the activation of the Keap1/Nrf2 signaling pathway.[44] These target proteins can regulate the oxidation–reduction balance in the body after activation. A study has shown that silver nanoparticles induce the activation of the stress response gene *Nrf2* in zebrafish.[45] In addition, ZnO NPs could upregulate *NQO-1* expression in the lungs of female mice.[46] Increased MDA content is associated with cell damage as a biomarker of oxidative stress.[47] In our study, the Keap1/Nrf2 signaling pathway was activated, and both MDA content and SOD activity were altered, indicating that the toxic effects of ZnO NPs may be related to the induction of oxidative stress and the destruction of the antioxidant enzyme system.

Nanoparticles induce ER stress.[6] The ER is an important site for protein synthesis.[48] The unfolded protein response (UPR), also known as ER stress, is activated when the organism is stimulated by an excessive buildup of misfolded or unfolded proteins.[49] Under normal conditions, ER transmembrane proteins require IRE1, PERK, and ATF6 to form

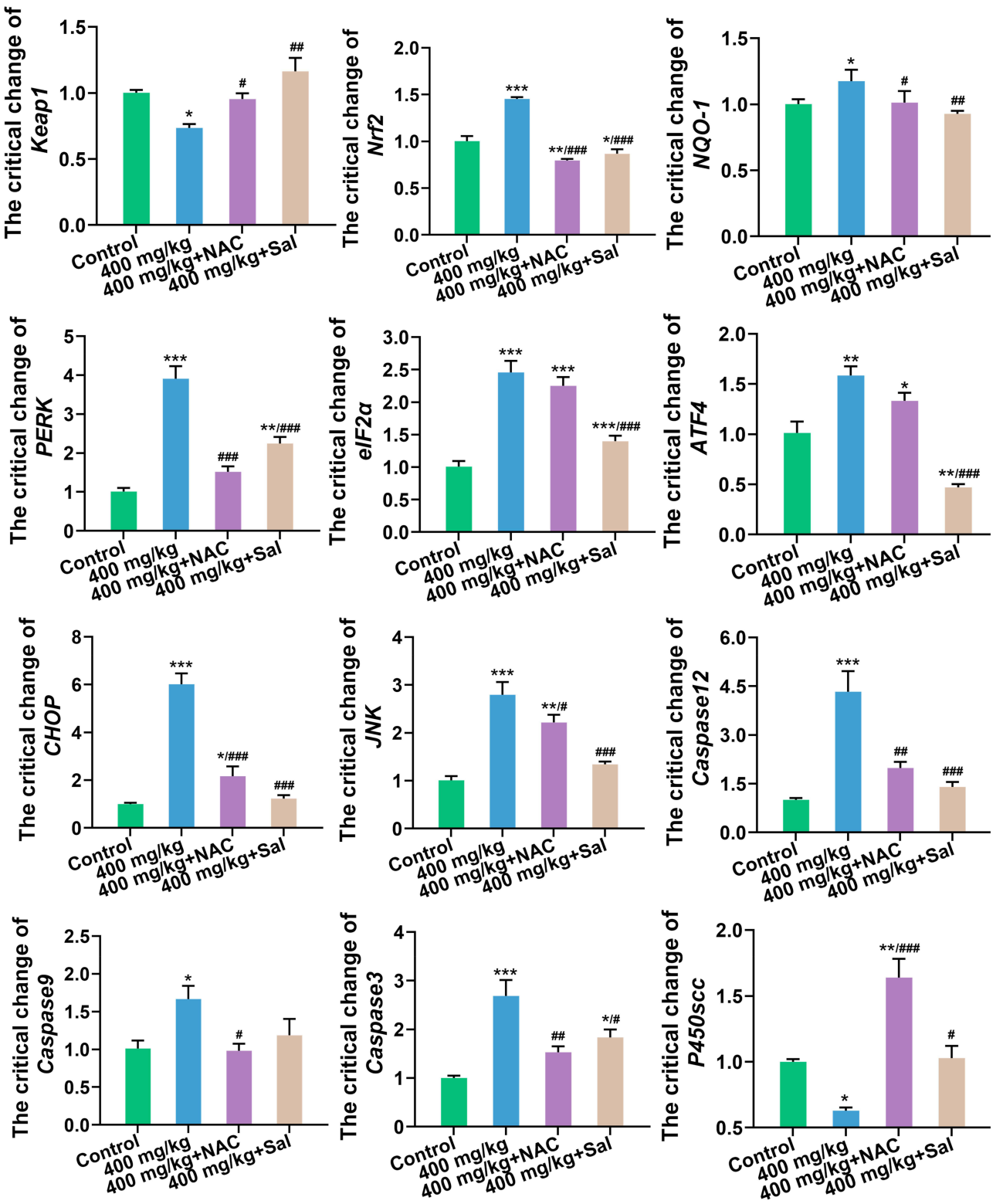

Figure 5 The expression levels of genes related to oxidative stress, ER stress, apoptosis and steroid hormone synthesis in ovary after the supplementation of NAC and Sal. *P < 0.05, **P < 0.01, ***P < 0.001: the 400 mg/kg ZnO NPs treatment group and the inhibitor groups versus the control group; #P< 0.05, ##P < 0.01, ###P < 0.001: the inhibitor groups versus the 400 mg/kg ZnO NPs treatment group.

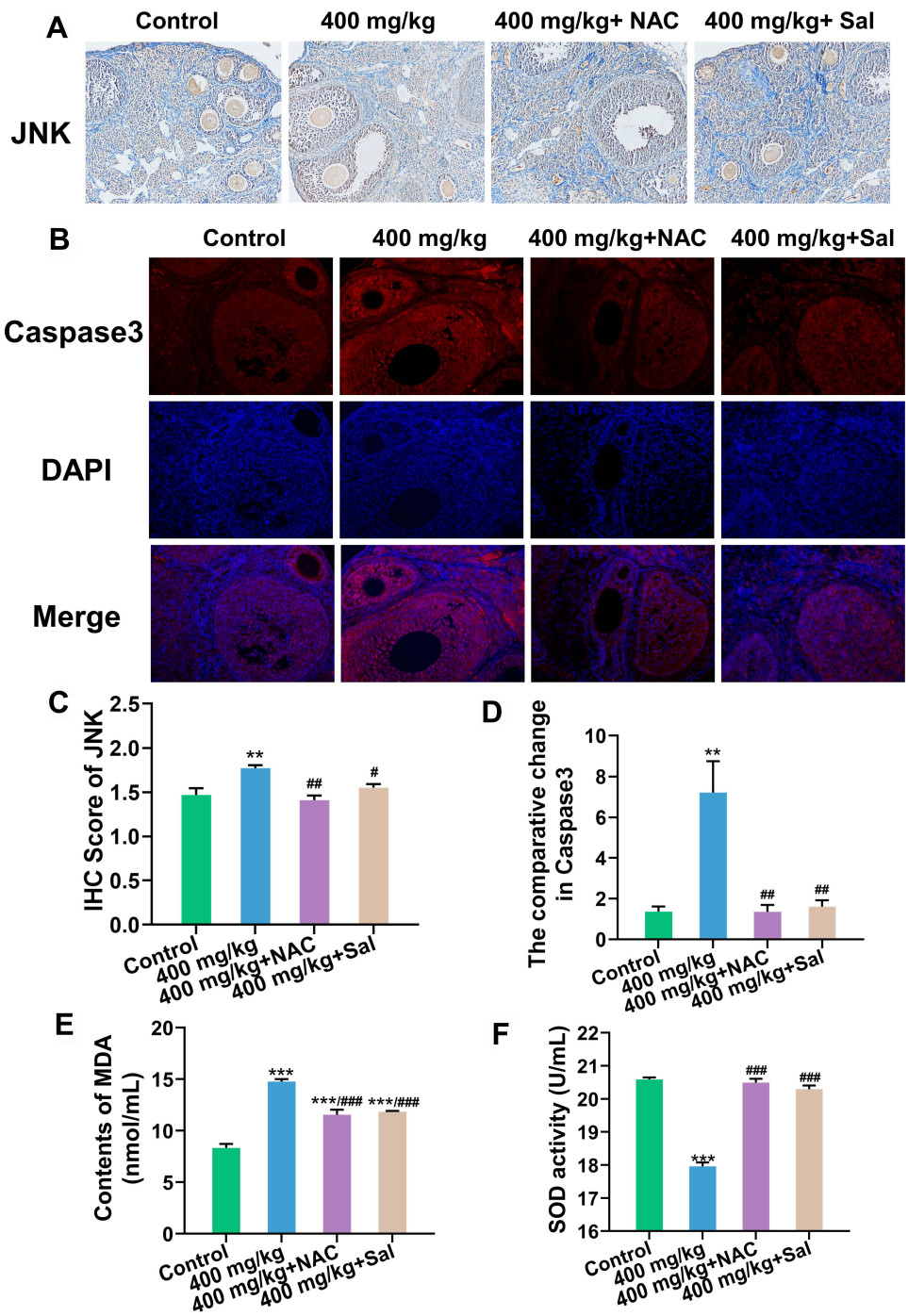

Figure 6 Protein expression of JNK and Caspase3 in ovary after the supplementation of NAC and Sal. (**A**) JNK expression detected by immunohistochemistry (IHC) (Magnification: ×200). (**B**) Caspase3 expression detected by immunofluorescence (IF) (Magnification: ×200). Blue: DAPI, red: Caspase3. (**C** and **D**) Semiquantitative analysis of JNK and Caspase3. (**E**) Content of MDA in serum. (**F**) SOD activity in serum. **P < 0.01, ***P < 0.001: the 400 mg/kg ZnO NPs treatment group and the inhibitor groups versus the control group; #P< 0.05, ##P < 0.01, ###P < 0.001: the inhibitor groups versus the 400 mg/kg ZnO NPs treatment group.

a stable complex with regulatory protein GRP78. After the abnormally excessive accumulation of ER proteins, these proteins dissociate from their corresponding regulatory proteins, thereby activating ER stress pathways, including the PERK/eIF2α/ATF4 pathway. When the UPR is activated, PERK autophosphorylation promotes the phosphorylation of the translation initiation factor eIF2α, which leads to the upregulation of ATF4 expression.[50] When the stress response cannot be alleviated, apoptosis is induced through a variety of pathways, including CHOP, JNK and the caspase family.[24]

The critical changes of these genes in the present study indicated that the toxic effects on the ovary may be strongly related to ER stress, which induces apoptosis.

The toxicity of ZnO NPs is dose-dependent. When the dosage of ZnO NPs increased gradually, the activation degree of oxidative stress, ER stress and other pathways in the body increased gradually, leading to the gradual deterioration of body damage. This occurrence has been shown in several studies.[6,25,31]

NAC is the acetylated form of cysteine, a precursor of reduced glutathione, which is known as a potent and commonly used inhibitor of oxidative stress. An in vivo experiment showed that the intraperitoneal injection of NAC can alleviate the follicular atresia and granulosa cell cycle arrest induced by advanced oxidation protein products.[51] Mahmoodi et al found that NAC could improve the function of ovarian grafting and follicular survival in mice by inhibiting oxidative stress.[52] Chinese scholars also found that NAC can regulate Keap1/Nrf2 signaling via miR-141 to improve prostatitis.[53] In addition to its antioxidant effects, NAC also has a metal-chelating capability.[54] However, the toxicity of ZnO NPs is due to Zn^{2+} and NPs in various investigations.[55,56] Therefore, the effect of metal chelation by NAC on the results was not further considered in this study. Sal is a selective dephosphorylation inhibitor of eIF2α. It specifically targets the PERK/eIF2α/ATF4 signaling pathway. Sal inhibits ER stress, and thus alleviates rotenone-induced neuronal injury.[57] In addition, Sal could ameliorate chronic hyperalgesia in mice with sickle cell via reducing ER stress.[58] As a result, NAC and Sal were administered to mice treated with ZnO NPs in this work to further validate the possible mechanism of ZnO NPs on mouse ovarian toxicity. The results revealed that NAC and Sal showed considerable inhibitory effects on the oxidative stress pathway and ER stress pathway, finally alleviating ovarian damage.

Conclusion

In this study, the toxic effects of ZnO NPs on the ovaries were investigated in female mice after a seven-day oral administration. Our results suggest that ZnO NPs had toxic effects on the ovary of female mice, which were due to oxidative stress, ER stress, and the eventual activation of apoptosis, and that NAC and Sal could serve as antidotes for unintentional ZnO NPs ingestion. Further studies focusing on the effect of the metal chelating ability of NAC on the results should be performed for confirmation.

Acknowledgment

This work was supported by National Natural Science Foundation of China (81771658).

Disclosure

The authors report no conflicts of interest in this work.

References

1. Oleszczuk P, Czech B, Konczak M, et al. Impact of ZnO and ZnS nanoparticles in sewage sludge-amended soil on bacteria, plant and invertebrates. *Chemosphere*. 2019;237:124359. doi:10.1016/j.chemosphere.2019.124359
2. Paiva-Santos AC, Herdade AM, Guerra C, et al. Plant-mediated green synthesis of metal-based nanoparticles for dermopharmaceutical and cosmetic applications. *Int J Pharm*. 2021;597:120311. doi:10.1016/j.ijpharm.2021.120311
3. El-Hady MMA, Farouk A, Sharaf S. Flame retardancy and UV protection of cotton based fabrics using nano ZnO and polycarboxylic acids. *Carbohydr Polym*. 2013;92(1):400–406. doi:10.1016/j.carbpol.2012.08.085
4. Cho S, Lee B, Park W, Huang X, Kim DH. Photoperiodic flower mimicking metallic nanoparticles for image-guided medicine applications. *ACS Appl Mater Interfaces*. 2018;10(33):27570–27577. doi:10.1021/acsami.8b09596
5. Chinnapaiyan M, Selvam Y, Bassyouni F, et al. Nanotechnology, green synthesis and biological activity application of zinc oxide nanoparticles incorporated argemone mxicana leaf extract. *Molecules*. 2022;27(5):1545. doi:10.3390/molecules27051545
6. Hu H, Guo Q, Fan X, et al. Molecular mechanisms underlying zinc oxide nanoparticle induced insulin resistance in mice. *Nanotoxicology*. 2020;14(1):59–76. doi:10.1080/17435390.2019.1663288
7. Huang KL, Lee YH, Chen HI, Liao HS, Chiang BL, Cheng TJ. Zinc oxide nanoparticles induce eosinophilic airway inflammation in mice. *J Hazard Mater*. 2015;297:304–312. doi:10.1016/j.jhazmat.2015.05.023
8. Liu H, Yang H, Fang Y, et al. Neurotoxicity and biomarkers of zinc oxide nanoparticles in main functional brain regions and dopaminergic neurons. *Sci Total Environ*. 2020;705:135809. doi:10.1016/j.scitotenv.2019.135809
9. Garolla A, Pizzol D, Carosso AR, et al. Practical clinical and diagnostic pathway for the investigation of the infertile couple. *Front Endocrinol (Lausanne)*. 2020;11:591837. doi:10.3389/fendo.2020.591837
10. Vander Borght M, Wyns C. Fertility and infertility: definition and epidemiology. *Clin Biochem*. 2018;62:2–10. doi:10.1016/j.clinbiochem.2018.03.012
11. Farquhar CM, Bhattacharya S, Repping S, et al. Female subfertility. *Nat Rev Dis Primers*. 2019;5(1):7. doi:10.1038/s41572-018-0058-8

12. Drummond AE. The role of steroids in follicular growth. *Reprod Biol Endocrinol*. 2006;4(1):16. doi:10.1186/1477-7827-4-16
13. Santacruz-Marquez R, Gonzalez-De Los Santos M, Hernandez-Ochoa I. Ovarian toxicity of nanoparticles. *Reprod Toxicol*. 2021;103:79–95. doi:10.1016/j.reprotox.2021.06.002
14. Wang R, Song B, Wu J, Zhang Y, Chen A, Shao L. Potential adverse effects of nanoparticles on the reproductive system. *Int J Nanomedicine*. 2018;13:8487–8506. doi:10.2147/IJN.S170723
15. Kuang H, Zhang W, Yang L, Aguilar ZP, Xu H. Reproductive organ dysfunction and gene expression after orally administration of ZnO nanoparticles in murine. *Environ Toxicol*. 2021;36(4):550–561. doi:10.1002/tox.23060
16. Saber M, Hayaei-Tehrani RS, Mokhtari S, Hoorzad P, Esfandiari F. In vitro cytotoxicity of zinc oxide nanoparticles in mouse ovarian germ cells. *Toxicol In Vitro*. 2021;70:105032. doi:10.1016/j.tiv.2020.105032
17. Nagarajan M, Maadurshni GB, Tharani GK, et al. Exposure to zinc oxide nanoparticles (ZnO-NPs) induces cardiovascular toxicity and exacerbates pathogenesis - Role of oxidative stress and MAPK signaling. *Chem Biol Interact*. 2022;351:109719. doi:10.1016/j.cbi.2021.109719
18. Yang D, Zhang M, Gan Y, et al. Involvement of oxidative stress in ZnO NPs-induced apoptosis and autophagy of mouse GC-1 spg cells. *Ecotoxicol Environ Saf*. 2020;202:110960. doi:10.1016/j.ecoenv.2020.110960
19. Bayat M, Daei S, Ziamajidi N, Abbasalipourkabir R, Nourian A. The protective effects of vitamins A, C, and E on zinc oxide nanoparticles (ZnO NPs)-induced liver oxidative stress in male Wistar rats. *Drug Chem Toxicol*. 2021;1–10. doi:10.1080/01480545.2021.2016809
20. Chen R, Huo L, Shi X, et al. Endoplasmic reticulum stress induced by zinc oxide nanoparticles is an earlier biomarker for nanotoxicological evaluation. *ACS Nano*. 2014;8(3):2562–2574. doi:10.1021/nn406184r
21. Kang JA, Jeon YJ. How is the fidelity of proteins ensured in terms of both quality and quantity at the endoplasmic reticulum? Mechanistic insights into E3 ubiquitin ligases. *Int J Mol Sci*. 2021;22(4). doi:10.3390/ijms22042078
22. van Anken E, Bakunts A, Hu CA, Janssens S, Sitia R. Molecular evaluation of endoplasmic reticulum homeostasis meets humoral immunity. *Trends Cell Biol*. 2021;31(7):529–541. doi:10.1016/j.tcb.2021.02.004
23. Cao T, Peng B, Zhou X, et al. Integrated signaling system under endoplasmic reticulum stress in eukaryotic microorganisms. *Appl Microbiol Biotechnol*. 2021;105(12):4805–4818. doi:10.1007/s00253-021-11380-1
24. Chen B, Hong W, Tang Y, Zhao Y, Aguilar ZP, Xu H. Protective effect of the NAC and Sal on zinc oxide nanoparticles-induced reproductive and development toxicity in pregnant mice. *Food Chem Toxicol*. 2020;143:111552. doi:10.1016/j.fct.2020.111552
25. Tang Y, Chen B, Hong W, et al. ZnO nanoparticles induced male reproductive toxicity based on the effects on the endoplasmic reticulum stress signaling pathway. *Int J Nanomedicine*. 2019;14:9563–9576. doi:10.2147/IJN.S223318
26. Chen B, Hong W, Yang P, et al. Nano zinc oxide induced fetal mice growth restriction, based on oxide stress and endoplasmic reticulum stress. *Nanomaterials*. 2020;10(2):34.
27. Yang P, Hong W, Zhou P, Chen B, Xu H. Nano and bulk ZnO trigger diverse Zn-transport-related gene transcription in distinct regions of the small intestine in mice after oral exposure. *Biochem Biophys Res Commun*. 2017;493(3):1364–1369. doi:10.1016/j.bbrc.2017.09.165
28. Li X, Zhang Y, Li B, et al. Prebiotic protects against anatase titanium dioxide nanoparticles-induced microbiota-mediated colonic barrier defects. *NanoImpact*. 2019;14:100164. doi:10.1016/j.impact.2019.100164
29. Zhao Y, Liu S, Tang Y, You T, Xu H. Lactobacillus rhamnosus GG ameliorated long-term exposure to TiO2 nanoparticles induced microbiota-mediated liver and colon inflammation and fructose-caused metabolic abnormality in metabolism syndrome mice. *J Agric Food Chem*. 2021;69(34):9788–9799. doi:10.1021/acs.jafc.1c03301
30. Liu S, Tang Y, Chen B, et al. Inhibition of testosterone synthesis induced by oral TiO2 NPs is associated with ROS-MAPK(ERK1/2)-StAR signaling pathway in SD rat. *Toxicol Res (Camb)*. 2021;10(4):937–946. doi:10.1093/toxres/tfab077
31. Shen J, Yang D, Zhou X, et al. Role of autophagy in zinc oxide Nanoparticles-Induced apoptosis of mouse LEYDIG cells. *Int J Mol Sci*. 2019;20(16):4042. doi:10.3390/ijms20164042
32. Liu XQ, Zhang HF, Zhang WD, et al. Regulation of neuroendocrine cells and neuron factors in the ovary by zinc oxide nanoparticles. *Toxicol Lett*. 2016;256:19–32. doi:10.1016/j.toxlet.2016.05.007
33. Zhou J, Peng X, Mei S. Autophagy in ovarian follicular development and atresia. *Int J Biol Sci*. 2019;15(4):726–737. doi:10.7150/ijbs.30369
34. Efendic F, Sapmaz T, Canbaz HT, Pence HH, Irkorucu O. Histological and biochemical apoptosis changes of female rats' ovary by Zinc oxide nanoparticles and potential protective effects of l-arginine: an experimental study. *Ann Med Surg*. 2022;74:103290. doi:10.1016/j.amsu.2022.103290
35. Yu M, Sun X, Dai X, et al. Effects of tannic acid on antioxidant activity and ovarian development in adolescent and adult female Brandt's voles. *Reprod Sci*. 2021;28(10):2839–2846. doi:10.1007/s43032-021-00578-3
36. Yu H, Kuang M, Wang Y, et al. Sodium arsenite injection induces ovarian oxidative stress and affects steroidogenesis in rats. *Biol Trace Elem Res*. 2019;189(1):186–193. doi:10.1007/s12011-018-1467-y
37. Yu C, Jiang F, Zhang M, et al. HC diet inhibited testosterone synthesis by activating endoplasmic reticulum stress in testicular Leydig cells. *J Cell Mol Med*. 2019;23(5):3140–3150. doi:10.1111/jcmm.14143
38. Hong F, Wang L. Nanosized titanium dioxide-induced premature ovarian failure is associated with abnormalities in serum parameters in female mice. *Int J Nanomedicine*. 2018;13:2543–2549. doi:10.2147/IJN.S151215
39. Kaweeteerawat C, Ivask A, Liu R, et al. Toxicity of metal oxide nanoparticles in Escherichia coli correlates with conduction band and hydration energies. *Environ Sci Technol*. 2015;49(2):1105–1112. doi:10.1021/es504259s
40. Chen L, Wu H, Hong W, Aguilar ZP, Fu F, Xu H. The effect of reproductive toxicity induced by ZnO NPs in mice during early pregnancy through mitochondrial apoptotic pathway. *Environ Toxicol*. 2021;36(6):1143–1151. doi:10.1002/tox.23113
41. Liu H, Lai W, Liu X, et al. Exposure to copper oxide nanoparticles triggers oxidative stress and endoplasmic reticulum (ER)-stress induced toxicology and apoptosis in male rat liver and BRL-3A cell. *J Hazard Mater*. 2021;401:123349. doi:10.1016/j.jhazmat.2020.123349
42. Kessler A, Hedberg J, Blomberg E, Odnevall I. Reactive oxygen species formed by metal and metal oxide nanoparticles in physiological media-A review of reactions of importance to nanotoxicity and proposal for categorization. *Nanomaterials*. 2022;12(11):1922. doi:10.3390/nano12111922
43. Lee DY, Song MY, Kim EH. Role of oxidative stress and Nrf2/KEAP1 signaling in colorectal cancer: mechanisms and therapeutic perspectives with phytochemicals. *Antioxidants*. 2021;10(5):21.

44. Yang X, Wang W, Zhang Y, Wang J, Huang F. Moxibustion improves ovary function by suppressing apoptosis events and upregulating antioxidant defenses in natural aging ovary. *Life Sci*. 2019;229:166–172. doi:10.1016/j.lfs.2019.05.040
45. Tayemeh MB, Kalbassi MR, Paknejad H, Joo HS. Dietary nanoencapsulated quercetin homeostated transcription of redox-status orchestrating genes in zebrafish (Danio rerio) exposed to silver nanoparticles. *Environ Res*. 2020;185:109477. doi:10.1016/j.envres.2020.109477
46. Rossner P, Vrbova K, Strapacova S, et al. Inhalation of ZnO nanoparticles: splice junction expression and alternative splicing in mice. *Toxicol Sci*. 2019;168(1):190–200. doi:10.1093/toxsci/kfy288
47. Tsikas D. Assessment of lipid peroxidation by measuring malondialdehyde (MDA) and relatives in biological samples: analytical and biological challenges. *Anal Biochem*. 2017;524:13–30. doi:10.1016/j.ab.2016.10.021
48. Park WJ, Park JW. The role of sphingolipids in endoplasmic reticulum stress. *FEBS Lett*. 2020;594(22):3632–3651. doi:10.1002/1873-3468.13863
49. Eisvand F, Tajbakhsh A, Seidel V, Zirak MR, Tabeshpour J, Shakeri A. Quercetin and its role in modulating endoplasmic reticulum stress: a review. *Phytother Res*. 2022;36(1):73–84. doi:10.1002/ptr.7283
50. Chipurupalli S, Samavedam U, Robinson N. Crosstalk Between ER Stress, Autophagy and Inflammation. *Front Med*. 2021;8. doi:10.3389/fmed.2021.758311
51. Zhou XY, Zhang J, Li Y, et al. Advanced oxidation protein products induce G1/G0-phase arrest in ovarian granulosa cells via the ROS-JNK/p38 MAPK-p21 pathway in premature ovarian insufficiency. *Oxid Med Cell Longev*. 2021;2021:6634718. doi:10.1155/2021/6634718
52. Mahmoodi M, Soleimani Mehranjani M, Shariatzadeh SM, Eimani H, Shahverdi A. N-acetylcysteine improves function and follicular survival in mice ovarian grafts through inhibition of oxidative stress. *Reprod Biomed Online*. 2015;30(1):101–110. doi:10.1016/j.rbmo.2014.09.013
53. Wang LL, Huang YH, Yan CY, et al. N-acetylcysteine ameliorates prostatitis via miR-141 regulating Keap1/Nrf2 signaling. *Inflammation*. 2016;39(2):938–947. doi:10.1007/s10753-016-0327-1
54. Wolfram T, Schwarz M, Reuss M, et al. N-Acetylcysteine as modulator of the essential trace elements copper and zinc. *Antioxidants*. 2020;9(11). doi:10.3390/antiox9111117.
55. Zhang WD, Zhao Y, Zhang HF, et al. Alteration of gene expression by zinc oxide nanoparticles or zinc sulfate in vivo and comparison with in vitro data: a harmonious case. *Theriogenology*. 2016;86(3):850–861 e851. doi:10.1016/j.theriogenology.2016.03.006
56. Lopes S, Ribeiro F, Wojnarowicz J, et al. Zinc oxide nanoparticles toxicity to Daphnia magna: size-dependent effects and dissolution. *Environ Toxicol Chem*. 2014;33(1):190–198. doi:10.1002/etc.2413
57. Goswami P, Gupta S, Biswas J, et al. Endoplasmic reticulum stress plays a key role in rotenone-induced apoptotic death of neurons. *Mol Neurobiol*. 2016;53(1):285–298. doi:10.1007/s12035-014-9001-5
58. Lei J, Paul J, Wang Y, et al. Heme causes pain in sickle mice via toll-like receptor 4-mediated reactive oxygen species- and endoplasmic reticulum stress-induced glial activation. *Antioxid Redox Signal*. 2021;34(4):279–293. doi:10.1089/ars.2019.7913